EUROPEAN COMMISSION

Community Research

SEVENTH FRAMEWORK PROGRAMME

CARBOWASTE

Treatment and Disposal of Irradiated Graphite and Other Carbonaceous Waste

Grant Agreement Number: FP7-211333

Technical Report T-6.3.5
Encapsulation of TRISO particle fuel in durable soda-lime-silicate glasses

Author(s): **Paul G. Heath[1], Claire L. Corkhill[1], Martin C. Stennett[1], Russel J. Hand[1], Willem C.H.M. Meyer[2], Neil C. Hyatt[2]**

1) Immobilisation Science Laboratory, Department of Materials Science and Engineering
2) Necsa, South African Nuclear Energy Corporation

Reporting period: e.g. 01/04/2008– 31/01/2013

Date of issue of this report: 28/02/2013

Start date of project : **01/04/2008** Duration : **48 Months**

Project co-funded by the European Commission under the Seventh Framework Programme (2007 to 2011) of the European Atomic Energy Community (EURATOM) for nuclear research and training activities		
Dissemination Level		
PU	Public	
RE	Restricted to the partners of the CARBOWASTE project	
CO	Confidential, only for specific distribution list defined on this document	**X**

Distribution list

Person and organisation name and/or group	Comments
All Carbowaste Partners	
Coordinator	
European Commission	

CARBOWASTE		
Work package: 6 **Task: :** 6.3	**CARBOWASTE document no:** CARBOWASTE-1303-T-6.3.5	**Document type:** T=Technical Report
Issued by: NECSA (SA) **Internal no.: CW-6-3-5-T-b-NECSA-F**		**Document status:** Final

Document title

Encapsulation of TRISO particle fuel in durable soda-lime-silicate glasses

Executive summary

Tri-Structural Isotropic (TRISO) coated particle-fuel is a key component in designs for future high temperature nuclear reactors. This study investigated the suitability of three soda lime silicate glass compositions, for the encapsulation of simulant TRISO particle fuel. A cold press and sinter (CPS) methodology was employed to produce TRISO particle–glass composites. Composites produced were determined to have an aqueous durability, fracture toughness and Vickers' hardness comparable to glasses currently employed for the disposal of high level nuclear wastes. Sintering at 700 C for 30 min was found to remove all interconnected porosity from the composite bodies and oxidation of the outer pyrolytic carbon layer during sintering was prevented by processing under a 5% H2/N2 atmosphere. However, the outer pyrolytic carbon layer was not effectively wetted by the encapsulating glass matrix. The aqueous durability of the TRISO particle–glass composites was investigated using PCT and MCC-1 tests combined with geochemical modelling. It was found that durability was dependent on silicate and calcium solution saturation. This study provides significant advancements in the preparation of TRISO particle encapsulant waste forms. The potential for the use of non-borosilicate sintered glass composites for TRISO particle encapsulation has been confirmed, although further refinements are required.

Revisions

Rev.	Date	Short description	Author	Internal Review	Task Leader	WP Leader
00	dd/mm/yyyy	Issue	Name, Organisation	Name, Organisation *Signature*	Name, Organisation *Signature*	Name, Organisation *Signature*
01	30/03/2013	First issue	P.G. Heath INL (UK)	N.C. Hyatt NECSA	W.C.H.M. Meyer NECSA	B. Grambow, SUBATECH

ARTICLE IN PRESS

Journal of Nuclear Materials xxx (2013) xxx–xxx

Contents lists available at SciVerse ScienceDirect

Journal of Nuclear Materials

journal homepage: www.elsevier.com/locate/jnucmat

Encapsulation of TRISO particle fuel in durable soda-lime-silicate glasses

Paul G. Heath [a], Claire L. Corkhill [a], Martin C. Stennett [a], Russell J. Hand [a], Willem C.H.M. Meyer [b], Neil C. Hyatt [a,*]

[a] Immobilisation Science Laboratory, Department of Materials Science and Engineering, Robert Hadfield Building, University of Sheffield, Sheffield S1 3JD, United Kingdom
[b] Necsa, South African Nuclear Energy Corporation, PO Box 582, Pretoria, Gauteng, South Africa

GRAPHICAL ABSTRACT

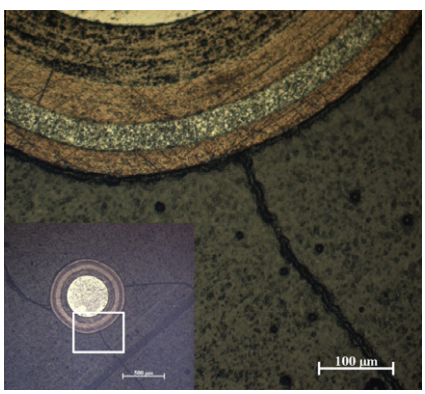

ARTICLE INFO

Article history:
Received 26 September 2012
Accepted 4 January 2013
Available online xxxx

ABSTRACT

Tri-Structural Isotropic (TRISO) coated particle-fuel is a key component in designs for future high temperature nuclear reactors. This study investigated the suitability of three soda lime silicate glass compositions, for the encapsulation of simulant TRISO particle fuel. A cold press and sinter (CPS) methodology was employed to produce TRISO particle–glass composites. Composites produced were determined to have an aqueous durability, fracture toughness and Vickers' hardness comparable to glasses currently employed for the disposal of high level nuclear wastes. Sintering at 700 °C for 30 min was found to remove all interconnected porosity from the composite bodies and oxidation of the outer pyrolytic carbon layer during sintering was prevented by processing under a 5% H_2/N_2 atmosphere. However, the outer pyrolytic carbon layer was not effectively wetted by the encapsulating glass matrix. The aqueous durability of the TRISO particle–glass composites was investigated using PCT and MCC-1 tests combined with geochemical modelling. It was found that durability was dependent on silicate and calcium solution saturation. This study provides significant advancements in the preparation of TRISO particle encapsulant waste forms. The potential for the use of non-borosilicate sintered glass composites for TRISO particle encapsulation has been confirmed, although further refinements are required.

© 2013 Elsevier B.V. All rights reserved.

1. Introduction

The most promising Generation IV nuclear reactor concepts are High Temperature Reactors (HTRs), such as the 'pebble bed' reactor and the US next generation nuclear plant. The advantages of these systems include passive safety mechanisms, production of direct process heat for industrial applications, online refuelling, and an increase in thermodynamic efficiency [1]. The use of multi layered spherical Tri-Structural Isotropic (TRISO) particle-fuel [2] is common to these reactor designs. TRISO particles have been engineered to be mechanically robust, corrosion resistant,

* Corresponding author. Tel.: +44 01142225470.
E-mail address: n.c.hyatt@sheffield.ac.uk (N.C. Hyatt).

0022-3115/$ - see front matter © 2013 Elsevier B.V. All rights reserved.
http://dx.doi.org/10.1016/j.jnucmat.2013.01.285

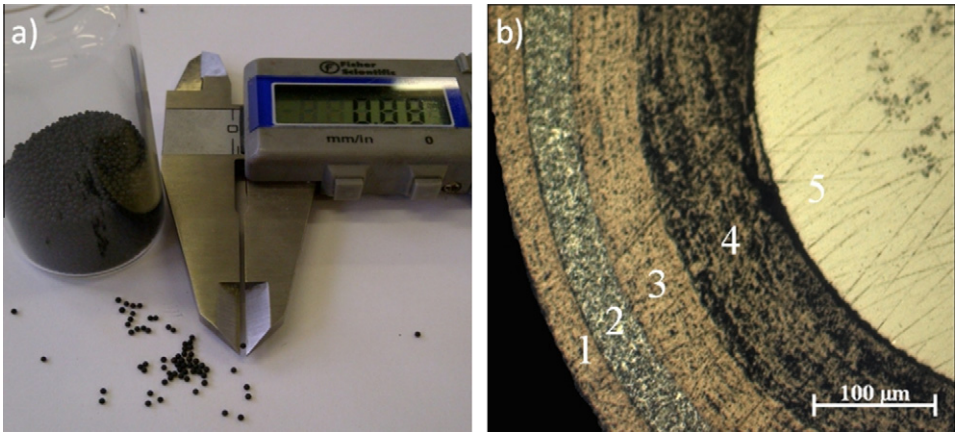

Fig. 1. (a) TRISO particles (micrometer display 0.88 mm) and (b) Sectioned TRISO particle illustrating the four functional layers and the central core: (1) OPyC, (2) SiC, (3) IPyC, (4) BC and (5) "UO_2" core (image displays zirconia surrogate core).

dimensionally stable at high temperatures and have the ability to retain fission products not only under normal operating conditions, but also under envisioned accident scenarios [3].

A TRISO particle consists of a spherical central core of UO_2 fuel coated with four functional layers as shown in Fig. 1. Moving inward toward the central UO_2 core (5), these protective layers are composed of: (1) an 'outer' pyrolytic carbon layer (OPyC), (2) a layer of silicon carbide (SiC), (3) an 'inner' pyrolytic carbon layer (IPyC) and (4) a final layer of 'buffer' carbon (BC). These layers work in concert to produce the favourable characteristics described above [4]. TRISO particles have been mass produced to a high standard with a low failure rate, typically 0.003% [5]. Overall, these factors combine to make TRISO particles a feasible option for use in a commercial reactor. TRISO particles are planned to be deployed in one of two forms, either as graphite pebbles containing approximately 10,000–40,000 particles or in fuel rods filled with TRISO particles [2].

It has been suggested that graphitic TRISO particle fuel arrays could be suitable for direct disposal in a Geological Disposal Facility (GDF) for radioactive wastes [6]. However, radiolysis of surrounding ground water has been shown to have a pronounced deleterious effect on the aqueous durability of graphite [7]. The interconnected porosity within the fuel arrays and the potential release of the radioactive ^{14}C content through this route brings the proposed direct disposal pathway into question. The coating system (Fig. 1) is designed to prevent radioactive material release from exposed TRISO particles.

It has been considered that segregation of the spent fuel component (i.e. individual TRISO particles), from the fuel array would significantly reduce the volume of the High Level Waste (HLW) to be disposed of from HTR operations. Even with the highest envisaged loading of TRISO particles per fuel array, the separation of these components would provide a 60% reduction in the volume of HLW produced (calculated from data in [8]). In the context of spent nuclear fuels and HLW, the primary constraint on waste emplacement in a GDF is likely to be the heat output of waste packages which will determine the packing density and hence overall costs. Nevertheless, reducing the overall number and volume of HLW waste packages would of considerable benefit in terms of reducing the cost of waste emplacement and GDF construction [9,10].

With these two issues in mind, the development of a disposal strategy which minimises the volume of HLW for disposal and imposes an engineered barrier to radionuclide release, would prove beneficial for future TRISO particle-fuel deployment. This disposal strategy may also provide a disposal route for the existing stockpile of Buffered Isotropic (BISO) and TRISO particles. This stockpile is estimated at over 52 tons heavy metal equivalent worldwide [11]. A portion of this existing stockpile has already, or is intended to be, subjected to irradiation in prototype reactors in the UK, Germany, Japan, the USA and China [2,11–14]. The technology could also prove advantageous for a variety of other problematic graphitic waste streams, such as the graphite fragments produced during the dismantling of graphite moderated reactor cores and highly contaminated Advanced Gas cooled Reactor (AGR) sleeves.

In a glass composite waste form, degradation of the host matrix will lead to the waste coming into direct contact with the environment, promoting the release of radionuclides [15]. However, the OPyC coating of TRISO particles is expected to remain uncontaminated by fission product species during normal HTR operation and has a reasonably high aqueous durability. This makes radionuclide release less of a concern than for other uncoated encapsulant waste streams, however, in principle, only the most durable and compatible matrices should be considered for use as HLW encapsulants.

Previous work has focused on the use of borosilicate glasses for the encapsulation of TRISO particles [16]. The deleterious interaction of TRISO particles with a glass melt at high temperature was reported. Mixing TRISO particles directly with a glass melt resulted in low waste loadings, poor wetting of the glass to the fuel, and oxidation of the OPyC layer leading to large pores [15]. The oxidation of the OPyC results in the exposure of the SiC layer; which plays host to highly radioactive fission products species. It was suggested that a process utilising sintered glass provided a more successful encapsulation, as evidenced by the structural integrity, good coating properties, low porosity and lack of oxidative reaction of the OPyC layer [16].

Some promise has been shown in studies utilising reaction bonded silicon carbide ceramics to act as TRISO particle encapsulants [9]. However, the simulated waste form was relatively porous and the stability of the SiC ceramic phase as a whole depends on passivation provided by a thin layer of SiO_2, which cannot be relied upon as an encapsulating matrix over geological time frames in a radioactive environment.

An alternative approach to TRISO particle encapsulation proposed the use of a graphite–glass composite, comprising formation of a graphitic puck by hot uni-axial pressing followed by "encapsulation" with molten borosilicate glass [17]. Significant oxidation of the graphite, which could result in the release of radioactive $^{14}CO_2$ and ^{14}CO in the case of spent TRISO particles, proved problematic. The production method suggested powdering of the TRISO particles into a 1 μm powder to form the graphitic body. This size reduction may prove prohibitive in practical terms, since processing routes requiring size reduction and dust formation for fission

product bearing wastes are strongly discouraged on the grounds of potential dose to the operations workforce. Other recent work has focused on graphite matrices made from a mixture of powdered, irradiated graphite and TRISO particles [6]. A graphitic matrix containing TRISO particles was produced, the porosity was filled using borosilicate glass and a similar hot pressing methodology to that described above was used. However, at these high processing temperatures, further study into potential oxidative losses of graphite must be considered.

The current work aimed to investigate the encapsulation of TRISO particles in sintered glass matrices with high aqueous durability, to minimise waste volume and further stabilise the waste with respect to release of radionuclides. The high aqueous durability of Soda Lime Silicate (SLS) glasses make them ideal candidates for radioactive waste disposal [18]. Nevertheless, the high temperatures required to produce fluid melts usually prohibit their use, due to excessive volatilisation of fission products. Nevertheless, SLS glasses may be considered as potential encapsulants using sintering methodologies, due to the lower processing temperature required. Therefore, three simple SLS glasses were chosen as the basis of this study. Glass–TRISO particle composites were formed using the cold press and sinter methodology (CPS) to determine the feasibility of these glasses to act as waste encapsulants for TRISO particles; based on physical properties of the composite, contacting properties between the TRISO particles and the matrix, the degree of OPyC oxidation and the aqueous durability.

2. Materials and experimental

2.1. TRISO particle simulant

A non-active TRISO particle-fuel simulant supplied by the PBMR (South Africa) was used, employing a surrogate zirconia core in place of UO_2. The density of the simulant was measured using helium pycnometry as 2.6640 ± 0.0005 g cm^{-3} on an AccuPyc 1340 II pycnometer with 200 purges of the chamber, 50 cycles, an equilibration rate of 0.005 psig min^{-1} at 25 °C in a 1 cm^3 chamber and a fill pressure of 12.5 psi.

2.2. SLS glasses

Three different compositions of SLS glasses were prepared: SLSA, SLSB and SLSC (see Table 1 for compositions). Batches were produced using stoichiometric quantities of industrial grade reagents (SiO_2, $NaCO_3$, $CaCO_3$, H_3BO_3 and $(MgCO_3)_4{\cdot}Mg(OH)_2{\cdot}5H_2O$). 500 g batches were preheated in alumina crucibles overnight at 1100 °C, subsequently ramped to 1500 °C and maintained at this temperature for a 5 h period. The melt was poured into blocks and annealed at 525 °C for 1 h then cooled to room temperature at 1 °C min^{-1}. Glass powders were produced using a Temer ring and puck mill. These were sieved to collect the sub-75 μm fraction for use in pellet formation (see below). The mean particle size of the powdered glasses SLSA, SLSB and SLSC was measured as 37 ± 27 μm, 39 ± 30 μm and 31.64 ± 23 μm, respectively.

2.3. R7T7 glass

A 200 g batch of R7T7 glass was produced using stoichiometric quantities of analytical grade reagents (SiO_2, $NaCO_3$, $CaCO_3$, Li_2CO_3, $Al(OH)_3$, $(ZnCO_3)_2.(ZnOH_2)_3$, Zr_3CO_8, and H_3BO_3). The melt was produced in a mullite crucible by ramping to 900 °C at 3 °C min^{-1} and subsequently ramping to 1350 °C at 10 °C min^{-1} for a dwell period of 2 h. The melt was poured into steel blocks and annealed at 500 °C for 1 h then cooled to room temperature at 1 °C min^{-1}. An identical preparation and analytical procedure to that for the SLS glasses was performed. The mean powder particle size was determined to be 48 ± 33 μm.

Table 1
Properties of glasses used in study. Compositions stated as batched. Compositional data in squared brackets as analysed by X-ray fluorescence spectroscopy.

Glass component [analysed] (mol%)	Sample name			
	SLSA	SLSB	SLSC	R7T7
SiO_2	69.00 [68.23]	74.00 [74.86]	74.00 [76.76]	60.5 [53.29]
Na_2O	15.00 [13.31]	15.00 [12.73]	15.00 [13.04]	7.00 [5.81]
CaO	15.00 [12.90]	10.00 [8.70]	5.00 [4.52]	5.75 [4.34]
B_2O_3	1.00 [1.72]	1.00 [1.20]	1.00 [1.53]	16.1 [19.54]
Al_2O_3	– [1.75]	– [0.14]	– [0.71]	2.6 [8.32]
MgO	– [>0.03]	– [0.03]	5.00 [2.32]	– [0.07]
P_2O_5	– [>0.12]	– [>0.07]	– [>0.12]	– [>1.10]
Fe_2O_3	– [>0.13]	– [>0.08]	– [>0.13]	– [0.15]
SO_3	– [>0.07]	– [>0.04]	– [>0.07]	– [>0.06]
K_2O	– [>0.08]	– [>0.05]	– [>0.08]	– [0.3]
BaO	– [>0.13]	– [>0.08]	– [>0.13]	– [1.12]
Li_2O	– [>0.02]	– [>0.01]	– [>0.03]	5.3 [1.22]
ZnO	– [>0.07]	– [>0.04]	– [>0.07]	2.4 [3.7]
ZrO_2	– [>0.10]	– [>0.06]	– [>0.10]	0.35 [0.86]
Density (g cm^{-3})	2.578 ± 0.003	2.535 ± 0.003	2.486 ± 0.003	2.522 ± 0.003
TEC (10^{-6} K^{-1})	11.4 ± 0.2	11.2 ± 0.2	10.6 ± 0.2	8.62 ± 0.2
T_g (°C)	595 ± 5	583 ± 5	555 ± 5	527 ± 5

2.4. Pellet formation

Glass pellets (~2 g) were formed by uniaxially pressing powdered glass (as prepared above) in a 13 mm diameter die with a pressure of 3 tons. These were sintered between 650 °C and 750 °C for 15–60 min.

2.5. Characterisation methods

The amorphous nature of the glasses was confirmed using X-ray powder diffraction on a Siemens D500 diffractometer (Cu Kα radiation, over the range 10° < 2θ < 60°, step size 0.02°, 0.6° 2θ min^{-1}). Densities of the glasses were determined using helium pycnometry in powder form as described above. Results are shown in Table 1.

Glass transition temperature (T_g) was determined using Differential Thermal Analysis performed on a Perkin Elmer DTA 7, data were acquired over the range 25–1000 °C at a rate of 10 °C min^{-1}. The glass transition was determined by the extrapolation of tangents at the point of interest using the Netzsch Pyris software package. Compositional analysis was performed using X-ray Fluorescence Spectroscopy (XRF) on a Phillips PW2404 XRF Axios.

A glass monolith with dimensions of 5 × 5 × 15 mm was cut using a diamond edged slow saw for dilatometry. This was performed on a Netzsch DIL 402C dilatometer from 25 to 300 °C with a heat rate of 2 °C min^{-1} and the thermal expansion co-efficient was determined using Netzsch Proteus software.

Particle size was determined using a Coulter LS130 particle analyser set at 45% PIDS and 7% obscuration. Sonication was applied during loading, run and interval, and results averaged over 15 runs of 120 s each and calculated with the Fraunhoffer optical model, including PIDS conditions.

2.6. Glass–TRISO particle composite preparation and analysis

Composite pellets were formed by an identical process to that described above, with the addition of 10 wt% of TRISO particle simulant mixed with the three different glass powders. Pellets and composites were sintered in a tube furnace under either air or in a reducing atmosphere of 5% H_2/N_2, at 650–750 °C for 15–60 min. X-ray diffraction was performed on the sintered glass pellets (parameters as above) to confirm their amorphous nature. Sintered composites were sectioned with a diamond edged slow saw, resin mounted, ground and polished to a 1 μm finish for examination with optical microscopy. Grinding was performed using 600 and 1000 grit diamond matrix plates and polishing using diamond pastes. Optical microscopy was performed on a Reichert–Jung Polyvar Met microscope equipped with a Zeiss AxioCam MRc.

Vickers' indentation was used to determine hardness (H_v) and fracture toughness (K_c) following the procedure described in [19]. Indentation was performed on a Mitutayo HM-101. Thirty indents were made at each of three indentation loadings, 1.96 N, 4.91 N and 9.81 N (10 indents at each force per sample, error ± 0.02 N). The load was held for 20 s. Samples were left for 24 h prior to analysis using optical microscopy (performed as above). The results quoted are those obtained from the 9.81 N loading due to the higher number of acceptable indentations (a minimum of five per sample).

Vickers' hardness (H_v) in Pa was calculated using the following equation:

$$H_v = \frac{1.854P}{(2a)^2} \quad (1)$$

where P is the load in Newtons, and $2a$ is the average diagonal length of the impression in m.

Fracture toughness (K_c) was calculated using the following equation:

$$K_c = \frac{0.0824P}{c^{3/2}} \quad (2)$$

where c is half the average crack length in m.

2.7. Dissolution experiments

Durability assessment of the glass materials was carried out on powdered SLSA, SLSB, SLSC composites and R7T7 sintered pellets. The assessment followed the procedure of ASTM standard C 1285-02 Product Consistency Test (PCT) using pure water at 90 °C in Teflon pots [20] and samples with a surface area to volume ratio between 2085 and 2160 m^{-1} (dependent on glass density for 75–150 μm glass fraction, see Table 1). Leachate samples were analysed for B, Ca, Na and Si concentrations using a Perkin–Elmer Optima 5300 dual view ICP-AES instrument (maximum error, 3× Standard Deviation (S.D.), below 5%).

Normalised mass losses were calculated according to the following equation:

$$\mathrm{NL}(i) = \frac{C_i \times f_c}{F_i \times \frac{\mathrm{SA}}{\mathrm{V}}} \quad (3)$$

where NL(i) is the normalised mass loss of element i (g m^{-2}), C_i is concentration of element in solution (g m^{-3}), f_c is element-oxide conversion factor (f_c = oxide molar mass (MO_x)/element molar mass), F_i is mass fraction of element oxide in glass and SA/V is the ratio of glass surface area to the volume of water (m^{-1}).

Normalised dissolution rates (NR(i), in g m^{-2} day^{-1}) were calculated according to the following equation:

$$\mathrm{NR}(i) = \frac{C_i \times f_c}{F_i \times \frac{\mathrm{SA}}{\mathrm{V}} \times t} \quad (4)$$

where t is the time of each sampling period in days.

The durability of the SLSA–TRISO particle composites sintered at 700 °C for 30 min was assessed following the procedure for ASTM standard C 1220-98 MCC-1 test [21] at 90 °C using pure water in Teflon pots with samples with a surface area to volume ratio of 10 m^{-1}. Aqueous elemental concentrations were determined by ICP-MS, performed using an Agilent 7500cx (maximum error, 3× Standard Deviation (S.D.), below 5%). The experimental method deviated from the ASTM standard as cylindrical rather than cuboidal monoliths were used. The surface area of the composite pellets was calculated geometrically using the Image J software package. Scaled images were taken of both the faces of the cylinder, which were used to calculate the surface area and circumference of each face. The thickness of the pellets was measured using a micrometer. Normalised mass losses were calculated as for the PCT test experiment.

2.8. Geochemical modelling

Analysis of the PCT and MCC-1 test data for SLSA was performed using the geochemical modelling software PHREEQC [22] using the PCHatches database. Aqueous elemental concentrations and pH data from the test leachates were modelled to determine relative saturation indices of potential equilibrium phases.

3. Results

The chemical compatibility of the glasses and TRISO particle simulant (i.e. the degree to which the OPyC is oxidised to form gaseous CO_2) was evaluated by sintering composites of each formulation at 700 °C for 6 h in both air and a reducing N_2/H_2 atmosphere. When sintering under air there was a complete oxidative reaction of the OPyC layer, resulting in the exposure of the SiC layer as displayed in Fig. 2a. The use of a reducing atmosphere eliminated this oxidative reaction (Fig. 2b). The OPyC remained completely intact under a reducing 5% H_2/N_2 atmosphere, even when sintered for several hours.

Sintering regimes yielding near-full density compacts of the SLS glass composites were determined. Potential oxidation of the OPyC at prolonged times required consideration, such that the optimised regime would produce dense compacts in the shortest possible time using the lowest possible temperature. TRISO particle-free pellets were sintered under an N_2/H_2 atmosphere at three sintering temperatures (650 °C, 700 °C and 750 °C) and times (15, 30 and 60 min). The density of these sintered glass pellets was measured using the Archimedes method (precision of ±0.1% in quoted densities) to build the sintering and densification matrix shown in Fig. 3. Sintering at 600 °C for up to 1 h could not produce specimens in excess of 90% of theoretical glass density for all three formulations. Specimens sintered at 700 °C for 30 min produced sintered bodies in excess of 95% of theoretical density. The achievement of this level of densification is significant as it is indicative of the removal of the interconnected porosity from a sintered body [23]. Little improvement in densification was observed with increases in either the temperature or duration of processing (Fig. 3).

Glass–TRISO particle composites were produced for formulations SLSA, SLSB and SLSC by sintering at 700 °C for 30 min under a 5% H_2/N_2 atmosphere. Fig. 4 shows that composites of all three

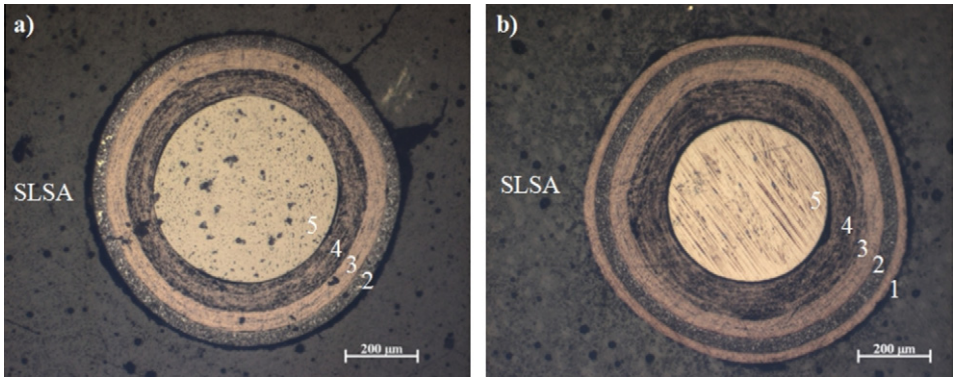

Fig. 2. TRISO particle–SLSA composites sintered in (a) air and (b) 5% H_2/N_2, illustrating the complete oxidation of the OPyC in air and the lack of oxidation under a reducing atmosphere.

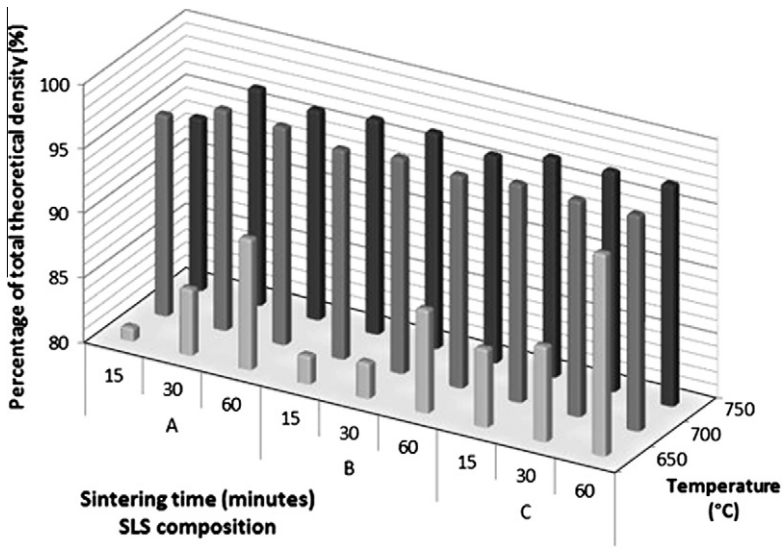

Fig. 3. Matrix displaying densification of SLS glasses under various time and temperature combinations (error below 1% of total measured density).

glass formulations showed near identical behaviour with respect to the oxidation of OPyC, wetting of TRISO particles by the matrix, and presence of residual porosity. Effective densification of all pellets was evidenced with a volume reduction between 25% and 30% (±5%). Oxidation of the OPyC in each composite was negligible as shown in Fig. 4a–f. The OPyC layer was found to have a constant thickness of 30 ± 5 µm both before and after encapsulation into sintered composites (150 measurements of the OPyC layer made across ten TRISO particles). The wetting of the glass to the OPyC layer was poor for all three formulations. A region of non-contact spanning up to 15 µm was apparent between the glass matrix and the OPyC as shown in Fig. 4d–f. The degree of wetting varied between particles as seen in Fig. 4c, however, no particle in any composite showed evidence of effective wetting over more than half its perimeter.

In composites of all three glasses, radial cracks emanated from the TRISO particles into the sintered glass matrix as shown in Figs. 4a–c and 5. These cracks were often interconnected, producing pathways to nearby particles, as shown in Fig. 4b. Residual porosity was retained in composites of all formulations as is displayed in Fig. 4g–i. Several of these pores were over 10 µm in size, yet this porosity did not appear to be interconnected, as is consistent with a measured density >95% of theoretical for the sintered glass compacts.

The comparable durability of the glasses when sintered at 700 °C for 30 min under 5% H_2/N_2 was assessed using the PCT methodology [20]. The durability of the French HLW base glass, R7T7, was also analysed by an identical methodology to allow comparison between SLS glasses and previous work on borosilicate glass formulations. The normalised mass loss for the PCT tests is shown in Fig. 6, with the change in the pH for these experiments given in Fig. 7 and the normalised dissolution rates given in Table 2.

The durability of the tested formulations based on normalised mass losses as determined by PCT were all within the same order of magnitude and increase in the following order from lowest to highest, SLSB < SLSC < SLSA < R7T7. The SLS formulations did not attain a steady state of dissolution for the glass network formers Si and B, as observed for the R7T7 formulation (Fig. 6). In the case of the SLS compositions, the normalised mass loss of network formers Si and B were lower than that for the modifier Na, and higher than that for the modifier Ca. The measured normalised mass loss for Ca decreased with time, suggesting that solution saturation of Ca was reached in all glasses. Buffering of leachate solutions for the three SLS-TRISO particle composites was similar reaching a pH of 11 after 3 days (Fig. 7). The R7T7 glass buffered to a lower pH of 10.

SLSA–TRISO particle composites were also studied using the MCC-1 method [21], to compare of the effects of dissolution in high and low surface area to volume ratio conditions. The results of this experiment are shown in Figs. 7 and 8, and Table 3. The MCC-1 test of formulation SLSA showed that the normalised mass loss of the

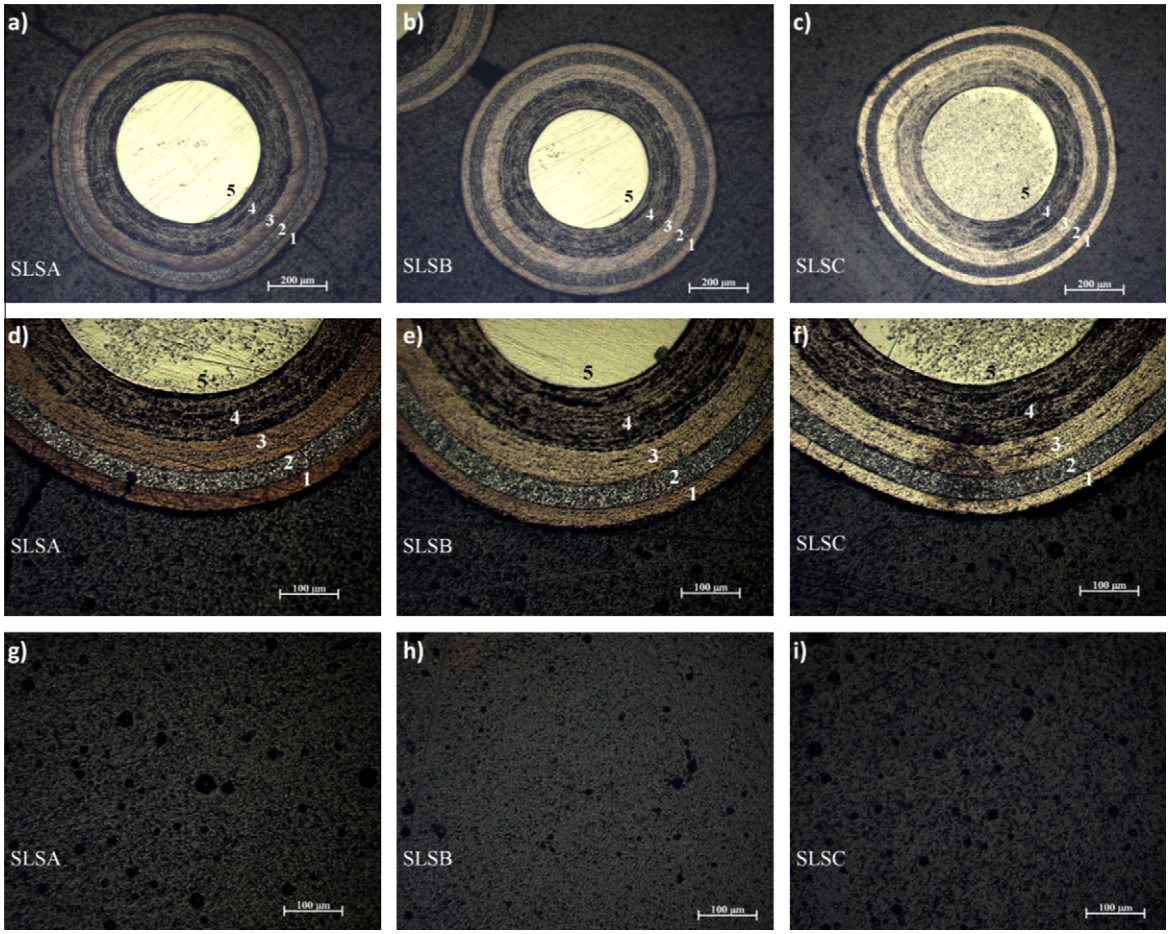

Fig. 4. Analysis of glass – TRISO particle composite pellets sintered at 700 °C for 30 min under an N_2/H_2 atmosphere of SLSA (a, d and g), SLSB (b, e and h) and SLS C (c, f and i). TRISO Particle and matrix integrity (a–c), wetting behaviour of matrix with the OPyC (d–f) and matrix porosity (g, h and i) are displayed.

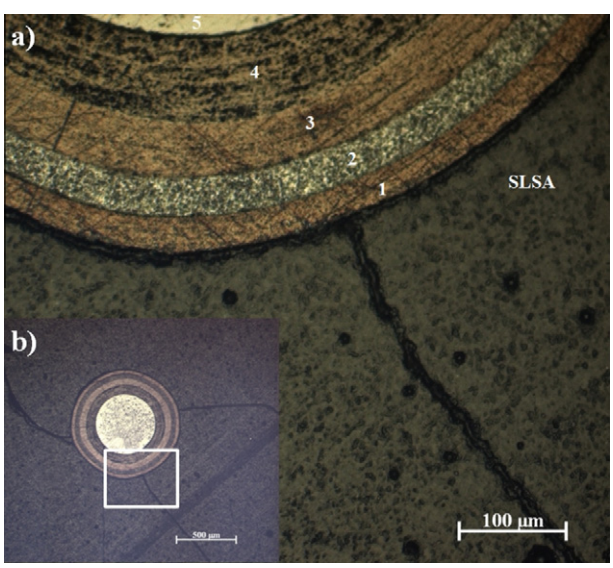

Fig. 5. Sintered SLSA–TRISO particle composite (a) close up of radial crack emanating from particle and (b) the same particle at a lower magnification displaying the extent of the damage to the glass matrix.

network modifier Ca was similar to that of Na. Normalised mass loss of network formers Si and B were significantly lower than that of the glass modifiers. Steady state dissolution rates did not appear to be reached for any element analysed (Fig. 8). Normalised dissolution rates were between 20 and 50 times higher than those measured for SLSA under the PCT conditions. The pH increased steadily during the experiment time to a maximum pH value of 9.4.

Geochemical modelling of the leachate resulting from SLSA dissolution tests under both PCT and MCC-1 regimes was conducted using PHREEQC. Saturation indices of phases which have been shown to be typically relevant to glass dissolution [24] are displayed in Fig. 9. The PCT leachates were determined to be further from solution saturation with respect to amorphous silica and H_3BO_3 than under the MCC-1 conditions. A number of calcium silicate phases were above the point of saturation in the leachates under the PCT conditions but not under the MCC-1 conditions.

Results for Vickers' hardness and fracture toughness are shown in Fig. 10 and Table 4. Vickers' hardness values of the glass–TRISO composites, across all formulations were comparable within precision. Fracture toughness measurements gave a spread of data with composites of SLSA and SLSB performing slightly better than SLSC and R7T7. All the sintered composites performed favourably in comparison with reported values of hardness and fracture toughness for HLW waste glasses currently deployed worldwide [19,25].

4. Discussion

With the exception of aqueous durability, little variation in the properties of interest were determined between the SLS formulations. The characteristics of chemical compatibility, porosity, wetting and radial cracking were similar across composites of formulations SLSA, SLSB and SLSC.

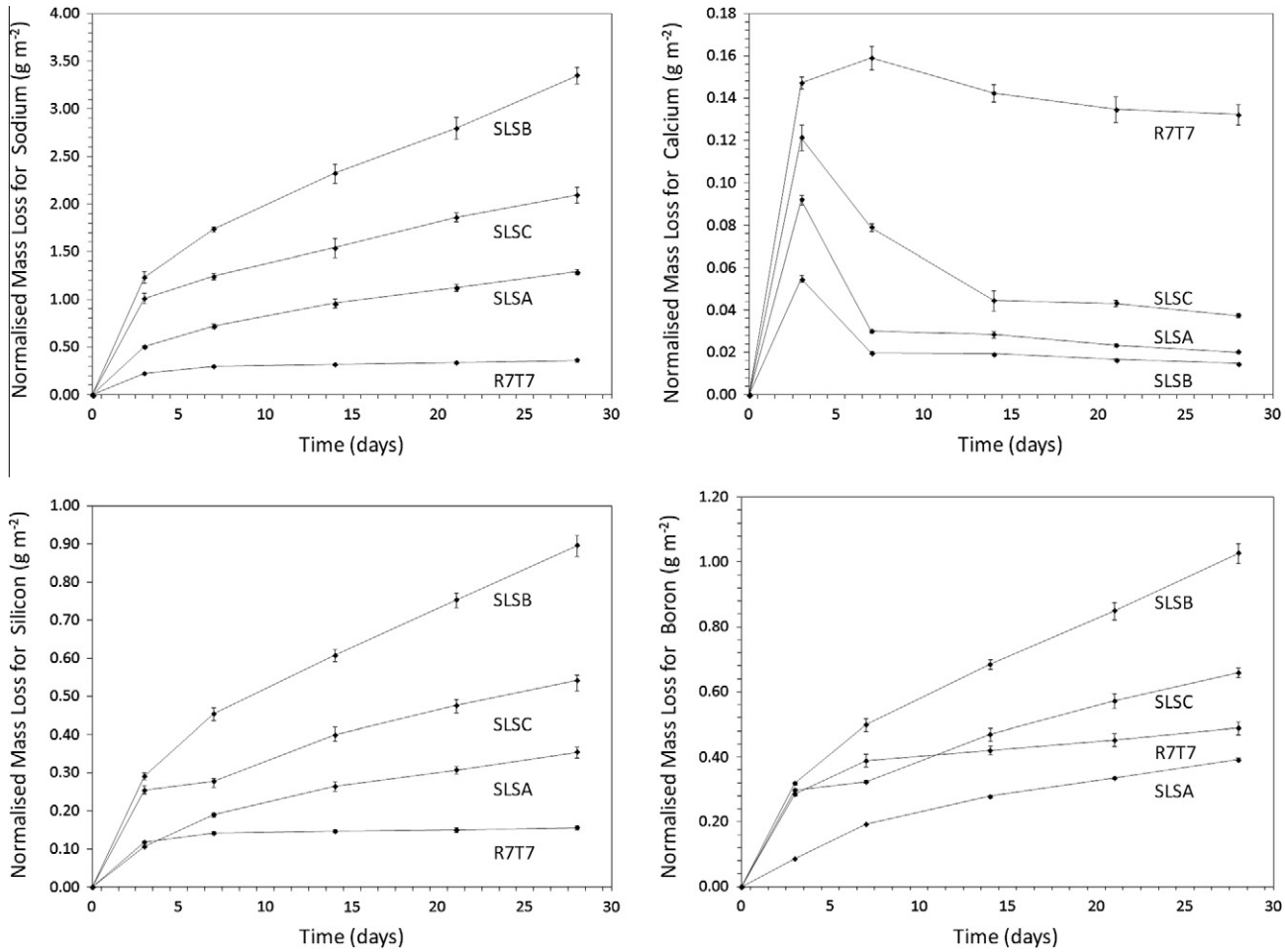

Fig. 6. Normalised mass losses of elements from PCT aqueous durability testing (errors 3× standard deviation from ICP-AES).

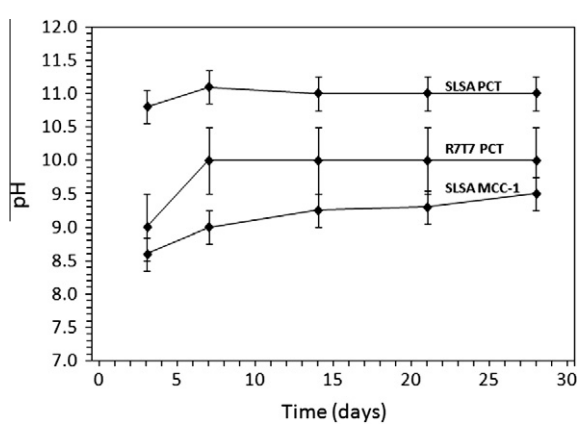

Fig. 7. Leachate solution pH throughout aqueous durability testing for sample SLSA tested under PCT and MCC-1 conditions, and for R7T7 tested under PCT conditions. Error bars are ±3× standard deviation.

4.1. OPyC oxidation

The SLS glasses studied as encapsulants for TRISO fuel show some promise for this purpose. Complete oxidation of the OPyC layer was observed when composites were sintered under air. This oxidation removes the outer protective layer of the TRISO particle, exposing the fission product-bearing SiC layer to the glass matrix. In the case of matrix degradation, the removal of this layer would help accelerate fission product release from the TRISO particle. As such, its retention in the waste form is desirable. We have demonstrated that this deleterious reaction between the matrix and OPyC can be easily avoided by sintering under a mildly reducing 5% H_2/N_2 atmosphere. This illustrates that the sintering atmosphere for the composite formation is an important factor and can be applied for glass formulations that may otherwise seem unsuitable for the encapsulation of TRISO particles. For example, altering the sintering atmosphere may allow the use of higher temperatures during processing which would be unacceptable under oxidising conditions.

The possibility of OPyC oxidation was further minimised through the study of sintering regimes. The shortest possible time and lowest temperature capable of producing compacts in excess of 95% theoretical density was determined to be 700 °C for 30 min, giving a densification that eliminated interconnected porosity in the sintered body. This is essential for reducing the surface area for dissolution, a key property for the geological disposal of radioactive waste forms.

4.2. TRISO particle–glass contacting behaviour

Wetting describes the behaviour of a liquid when the liquid contacts the surface of a solid. The use of the term in this context, to describe the matrix-TRISO particle interaction, may not be appropriate because it is not clear that the glass component is indeed liquid during sintering. As such, it may be more appropriate to refer to areas where matrix–TRISO particle interaction occurs as

Table 2
Normalised dissolution rates of elements at the end point of PCT aqueous durability tests (errors reported as ±3× standard deviation from ICP-AES).

Normalised dissolution rate at 28 days (g m^{-2} day^{-1})	Glass formulation			
	SLSA	SLSB	SLSC	R7T7
Si	0.0125 ± 0.0005	0.032 ± 0.001	0.0198 ± 0.0005	0.0128 ± 0.0002
B	0.0140 ± 0.0002	0.036 ± 0.001	0.0235 ± 0.0005	0.0174 ± 0.0007
Na	0.039 ± 0.001	0.096 ± 0.003	0.060 ± 0.003	0.0055 ± 0.0006
Ca	0.00070 ± 0.00005	0.00053 ± 0.00001	0.00136 ± 0.00003	0.0047 ± 0.0002

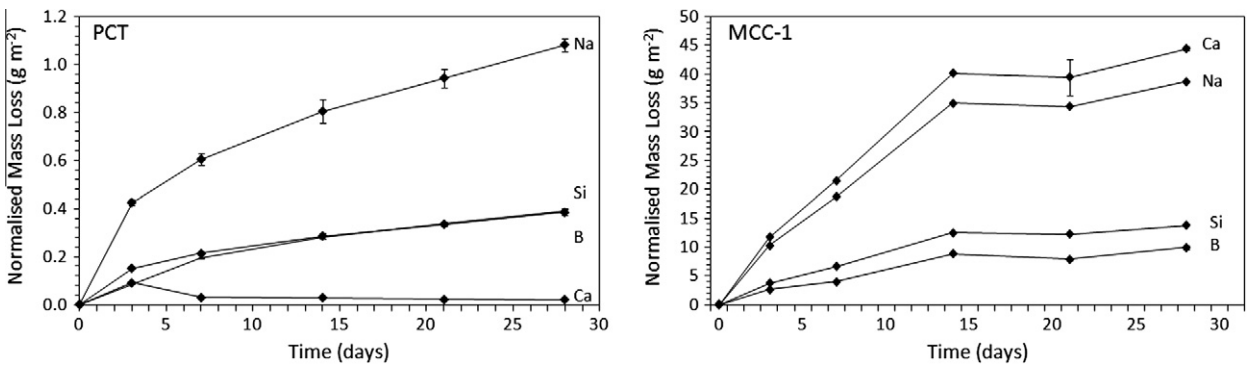

Fig. 8. Comparison between durability assessments of MCC-1 and PCT tests for SLSA (errors 3× standard deviation from ICP-AES and ICP-MS).

Table 3
PCT and MCC-1 rates of dissolution from normalised mass loss data after 28 days (errors reported as 3× standard deviation from ICP-AES and ICP-MS).

Element	Normalised dissolution rate at 28 days for SLSA (g m^{-2} day^{-1})	
	PCT	MCC-1
Si	0.0125 ± 0.0005	0.491 ± 0.008
B	0.0140 ± 0.0002	0.354 ± 0.005
Na	0.039 ± 0.001	0.69 ± 0.02
Ca	0.0007 ± 0.00005	0.033 ± 0.001

having 'contacting' behaviour promoted by sintering action, rather than 'wetting' *sensu stricto*. The existence of voids around the TRISO particles creates the potential for the whole surface area of the TRISO particles to be exposed as a consequence of dissolution or cracking of the encapsulating matrix. Therefore, the composite waste forms described in this study do not yet show the necessary coating of TRISO particles for a high quality waste form, whereby the encapsulant directly binds to the embedded material.

4.3. Glass composite aqueous durability

The aqueous durability of the sintered SLS glasses used for encapsulation is equivalent to that reported for similar commercial SLS glass [26]. This shows that the sintering process does not have a negative effect on the aqueous durability of the materials. The normalised release of network formers (Si and B) to solution is lower than that of modifier cation Na, as shown in Fig. 6, which indicates an ion exchange process in the corrosion mechanism.

The results show a marked difference in aqueous durability based on composite glass formulation. The release of most elements from SLSA is a factor of three smaller than that observed for SLSB and a factor of two smaller than that observed for SLSC (Fig. 6, Table 2). Due to the lower mole fraction of silica in SLSA, it was expected that this glass would have the lowest aqueous durability. However, the increased durability in SLSA may be explained by the greater alkali earth to alkali ratio, promoting cross linking in the glass network and blocking ion exchange pathways for sodium release [27]. The increased durability of SLSC relative to that of SLSB could also be a result of a mixed alkali earth effect

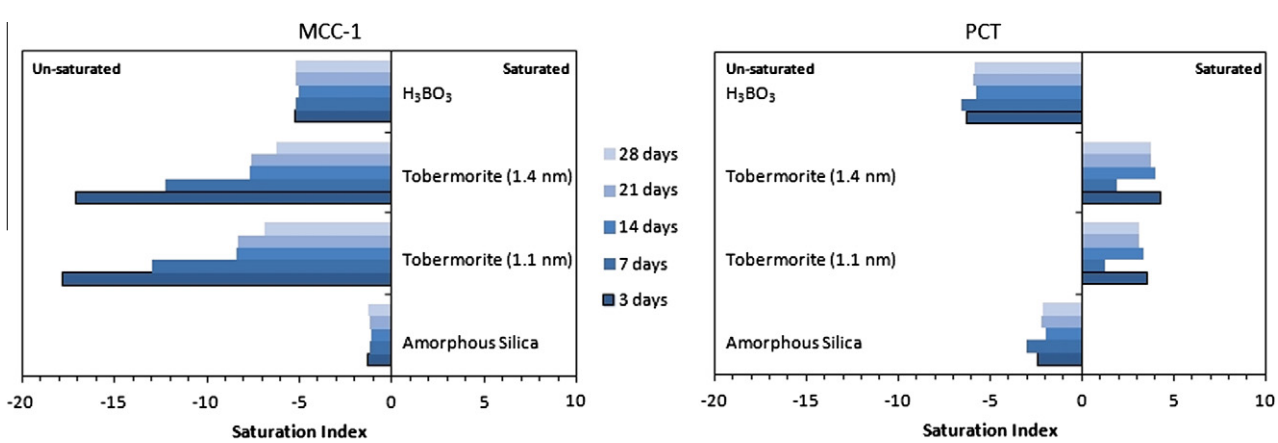

Fig. 9. Saturation indices of leachate solutions calculated using PHREEQC for SLSA under MCC-1 and PCT conditions.

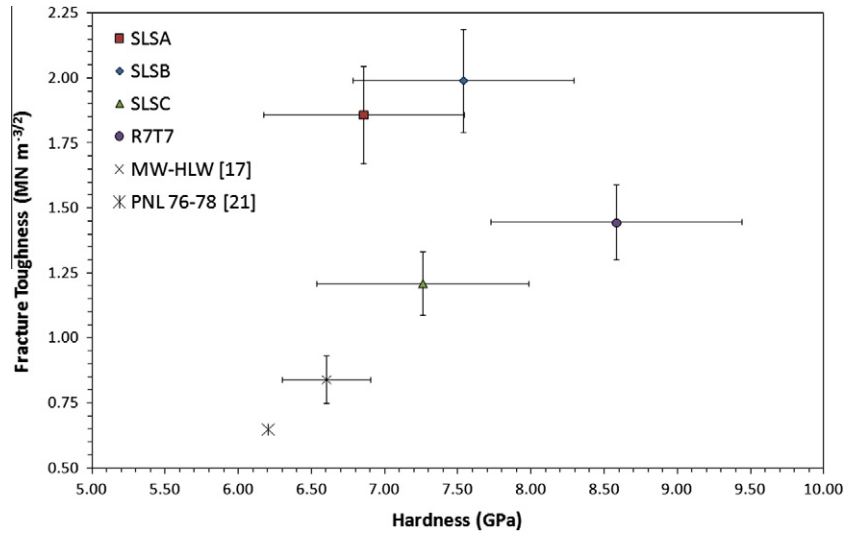

Fig. 10. Indentation fracture toughness *versus* hardness for sintered glass composites and comparison with previous HLW glass tests.

Table 4
Vickers' hardness and fracture toughness values for SLS glass composites and currently employed HLW glasses.

Glass formulation	Hardness at 1 kg loading (GPa)	Fracture toughness at 1 kg loading (M N $m^{-3/2}$)
SLSA	6.9 ± 0.7	1.9 ± 0.2
SLSB	7.5 ± 0.8	2.0 ± 0.2
SLSC	7.3 ± 0.8	1.2 ± 0.15
R7T7	8.6 ± 0.9	1.4 ± 0.15
MW-HLW [19]	6.6 ± 0.3	0.84 ± 0.09
PNL 76–78 [25]	6.2	0.65

[27]. The use of a mixture of alkali earth ions has been suggested to create a difference in cation field strength, significant enough to polarise non-bonding oxygen atoms in the glass structure [28]. This polarisation is thought to strengthen bonding between the cations and non-bonding oxygen atoms, thus decreasing diffusion of modifier cations from the structure, the rate of ion exchange and the rate of hydrolysis.

An alternative explanation for this behaviour may be provided by the presence of Al_2O_3 impurities in the glasses, most likely as a result of crucible corrosion. As shown in Table 1, the molar ratio of alumina increases in the same order as the aqueous durability (lowest to highest, SLSB < SLSC < SLSA). Additions of alumina have been shown previously to increase aqueous durability of SLS glasses [18] as discussed further below.

R7T7 borosilicate glass was tested using the identical methodology to that for the SLS composite glasses in the PCT test. The normalised mass loss of both silicon and boron in R7T7 over the 28 day test period was lower than those observed for any SLS composite glass tested. This result is contrary to what may be expected from a glass containing a significantly lower molar ratio of silica than the SLS composite formulations. It can be seen in Fig. 6 that after 7 days the normalised mass loss for boron, silicon and sodium in the R7T7 tests reaches a steady state. This may be indicative of solution saturation with respect to silicon, which can in turn slow or shut down the dissolution mechanism. A steady state of dissolution is not achieved for the SLS glass formulations even by the end of the 28 day test period.

The difference in attainment of steady state dissolution between the SLS composite formulations and R7T7 glass is likely due to leachate buffering effects creating differences in the pH, as shown in Fig. 7. The R7T7 glass buffers the solution to pH 10 within 3 days, while the SLS composite glasses buffer the test solution to pH 11 in the same time. The higher boron and aluminium content of the R7T7 glass (Table 1) buffers the solution according to Eqs. (5)–(7) [26–28].

$$(\equiv\text{Si—O})_y\text{B}^{3-y}(y-3)\text{Na}^+ + 3\text{H}_2\text{O} \rightarrow 3(\equiv\text{Si—OH}) + (y-3)(\equiv\text{Si—ONa}) + \text{H}_3\text{BO}_3 \quad (5)$$

$$\text{H}_3\text{BO}_3 + \text{H}_2\text{O} \rightleftarrows \text{B(OH)}_4^- + \text{H}^+ \quad (6)$$

$$\text{Al}_2\text{O}_3 + 2\text{OH}^- + 3\text{H}_2\text{O} \rightarrow 2[\text{Al(OH)}_4]^- \quad (7)$$

The dissolution of silicate glasses is well documented to be dependent on pH according to the term $10^{\sim 0.4\text{pH}}$ [29–32]. As such, the rate of glass dissolution at pH 11 is expected to be 2.5 times greater than at pH 10 with all other factors remaining constant. In addition, the solution saturation of silicon is ten times greater at pH 10.7 than at pH 10, due to the stabilisation of the silicate anion [33]. These factors combine to explain the differences in the dissolution profiles of the SLS composite and the R7T7 glasses.

In the ultimate disposal environment, the natural and manufactured materials in the near field and engineered disturbed zone will govern the buffered pH of the infiltrating groundwater, rather than the wasteform itself, depending on the flow rate. In the specific context of hypothetical co-disposal of UK HLW and ILW, utilising a cementitious backfill in the latter, which could lead to a hyperalkaline plume impacting the former, the self-imposed pH arising from dissolution of SLS glasses could be relevant.

Monolithic SLSA–TRISO particle composites were investigated using the MCC-1 durability test. This test produced a normalised leaching rate between 20 and 50 times greater (depending on the element) than that observed in the PCT test of SLSA (Table 3). It is well documented that increases in surface area to volume ratio lower the normalised mass loss of borosilicate glasses [34]. The larger surface area to volume ratio leads to enhanced dissolution rates and solution saturation with respect to silica. The process of glass dissolution in aqueous solution results in partial hydration of the glass network to form an amorphous layer of $SiO_{4-x}(OH)_x$. It has been suggested that this layer acts alongside precipitated phases such as calcium silicate hydrates (CSH), as a passivating barrier to minimise further dissolution [35–37], thus lowering the dissolution rate.

Geochemical modelling was performed in order to determine the presence and composition of potential alteration phases resulting from leaching of the PCT and MCC-1 samples. It must be noted that the results arising from this modelling are only as reliable as the thermodynamic data input to the model. However, comparison of two different thermodynamic databases provided similar results, where the solution was either significantly over- or under-saturated with respect to the mineral phases identified. This provides confidence in the predicted saturation indices of the potential alteration phases determined. In the SLSA composite glass, the solution was not found to be saturated with respect to amorphous silica for either type of test, as shown in Fig. 9, although the model indicates that the solution is closer to equilibrium for the MCC-1 test than the PCT test. This suggests that silica saturation is not the cause of the difference in normalised mass loss. Under PCT conditions a decrease in the normalised mass loss of calcium was observed with time for the SLSA composite, while the network formers B and Si were still being released into solution (Fig. 8). This is indicative of the precipitation of a calcium-bearing phase. No such effect was observed under MCC-1 conditions. Using geochemical modelling, it was found that the solution from the PCT experiment was far beyond the saturation limit for twelve of the twenty seven thermodynamically possible calcium bearing phases, including tobermorite ($Ca_5Si_6(O,OH)_{18}\cdot 5H_2O$), shown in Fig. 9. It has been suggested that tobermorite is a major constituent of CSH gel layers likely to exist in a glass alteration phase, which may passivate dissolution [23,35–37]. The MCC-1 test leachate was significantly under-saturated with respect to any of the Ca—Si phases contained in a CSH gel, including tobermorite (Fig. 9). Within the error limits of the thermodynamic data, we may infer that the enhanced dissolution rates in the MCC-1 test compared to the PCT test are the result of saturation with respect to calcium silicate phases in the PCT test.

It is possible that inaccuracies in the calculation of sample surface area may contribute to the observed results. The surface area of the composite pellets was measured geometrically. Cracks in the composite samples and the finish of the pellets exterior could not be accounted for using this determination of surface area, which may result in an under estimation of the surface area and, therefore an increase in the calculated normalised mass loss.

4.4. Physical properties

The Vickers' hardness and fracture toughness of the composite glasses and R7T7 were measured and found to be comparable with those found for HLW glasses currently employed for nuclear waste [19]. The results provided may be subject to some inaccuracy, as annealing the composite materials was precluded by the removal of the polished surface finish by sintering. It may be assumed that the mild compressive stresses created during polishing will have a positive effect on the values obtained for Vickers' hardness and fracture toughness. Nevertheless, trends in variation of Vicker's hardness are expected to be meaningful.

4.5. Suitability of SLS-glasses for TRISO particle encapsulation

The processing conditions described in this work have increased the compositional range of glasses which may be considered for use as TRISO particle encapsulants. Appropriate densification without oxidation of the OPyC layer is a significant advancement. The mechanical properties of Vickers' hardness and fracture toughness compared favourably to glasses currently employed as waste forms in radioactive waste management. However, it is clear that further refinements are required to improve several important characteristics. The contacting of the matrix to the TRISO particles is currently insufficient to form an effective coating and it has been shown that some residual porosity remains. This porosity does not appear to be interconnected; however, it remains an undesirable feature in a waste form for spent fuel due to the increased surface area it provides for aqueous dissolution. The determining characteristic of the glass composites, with respect to their potential use as TRISO particle encapsulants, is evidenced in the radial cracking emanating from the TRISO particles into the matrix. This is most likely a result of the mismatched thermal expansion coefficients of the TRISO particle and the glass matrix, increasing the susceptibility of the matrix to fracturing and therefore, increasing the surface area for leaching.

A compromise in durability and composite quality will likely have to be reached for the use of sintered silicate-based glasses as TRISO particle encapsulants. The issues identified could potentially be mitigated by increasing the mole fraction of B_2O_3 in the glass, as this would lower the thermal expansion coefficient, glass transition temperature and the viscosity, as such, preventing cracking, lowering processing temperatures and promoting contacting [38]. Alumina additions would likely have a positive effect both on aqueous durability and on lowering the thermal expansion coefficient. However, they also increase temperatures required for processing, as such, increasing potential risk of OPyC oxidation.

5. Conclusions

The SLS glasses studied showed some promise for the purpose of TRISO particle encapsulation. A simple alteration in the processing atmosphere was shown to allow the effective densification of glass–TRISO particle composites without an oxidative reaction of the OPyC layer. The mechanical properties of Vickers' hardness and fracture toughness compared favourably to glasses currently employed as waste forms in the nuclear industry. The mismatch between the thermal expansion coefficients of the glasses and TRISO particles proved detrimental to the waste form integrity. This mismatch resulted in the propagation of large radial cracks from the TRISO particle into the matrix. The contacting between TRISO particles and the glass matrix was also poor. These two issues currently preclude the use of CPS composites of these glass compositions as a waste form for TRISO particles.

The durability of the sintered SLS glasses was shown to be comparable to that of as-cast analogues known for their high durability. There was variation between glass formulations tested, likely a result of the mixed alkali effect and Al_2O_3 introduced during processing. Leachate pH was shown to have a dramatic effect on the dissolution of the glasses as seen by comparison with a borosilicate glass. Strong variations in normalised mass loss were observed for SLSA depending on the surface area to volume ratio of the test used. This is most likely a result of reaching saturation with respect to a calcium silicate phase in the leachate solution.

The results obtained show the potential of sintered glass composites for TRISO particle encapsulation, although the problems encountered here demonstrate the difficulties of increasing waste form durability. Determining factors in producing an effective waste form from sintered glasses will involve the matching of thermal expansion coefficients and providing an increased (long term) chemical durability.

Acknowledgements

The authors would like to thank Willie Meyer and the PBMR (South Africa) for the kind provision of TRISO particle simulant. The authors are grateful to Owen McGann and John Provis for their useful discussions. We thank EPRSC for part funding of this research under grant number EP/F055412/1 and the Nuclear FiRST Doctoral training centre under grant reference EP/G037140/1,

and University of Sheffield Knowledge Transfer Account, under grant reference EP/H500170/1. N. C. Hyatt is grateful to the Royal Academy of Engineering and the Nuclear Decommissioning Authority for funding.

References

[1] E. Cartlidge, Nuclear's New Generation, Physics World, Institute of Physics, 2010.
[2] A.W. Mehner, W. Heit, K. Röllig, H. Ragoss, H. Müller, J. Nucl. Mater. 171 (1990) 9–18.
[3] W. Schenk, A. Naoumidis, H. Nickel, J. Nucl. Mater. 124 (1984) 25–32.
[4] B. Liu, T. Liang, C. Tang, Rare Met. 25 (2006) 337–342.
[5] G.K. Miller, D.A. Petti, D.J. Varacalle, J.T. Maki, J. Nucl. Mater. 317 (2003) 69–82.
[6] J. Fachinger, K.H. Grosse, M. Hrovat, R. Seemann, Nucl. Eng. Des. 251 (2012) 235–238.
[7] J. Fachinger, M. den Exter, B. Grambow, S. Holgersson, C. Landesman, M. Titov, T. Podruhzina, Nucl. Eng. Des. 236 (2006) 543–554.
[8] H. Nabielek, G. Kaiser, H. Huschka, H. Ragoss, M. Wimmers, W. Theymann, Nucl. Eng. Des. 78 (1984) 155–166.
[9] A.A.B. Grambow, D. Grenèche, M.H. Mouliney, J. Fachinger, M. Titov, A. Bukaemsky, S. Neumann, Study of various options for final disposal of HTR coated particles, in: 3rd International Topical Meeting on High Temperature Reactor Technology, HTR 2006, Johannesburg, South Africa. October 1–4, 2006.
[10] IAEA, Technical, Institutional and Economic Factors Important for Developing a Multinational Radioactive Waste Repository, International Atomic Energy Agency, 1998.
[11] H.N.K. Verfondern, J.M. Kendall, Nucl. Eng. Technol. 39 (2007) 603–616.
[12] Draft Strategy for Consultation (September 2010), Nuclear Decommisioning Authority, 2010, pp. 29.
[13] T. Goddard, A Future for Nuclear Power, Physics World, Institute of Physics, 2006.
[14] D.K.J.R.C. Gough, J. Nucl. Energy 21 (1967) 623–642.
[15] I.W. Donald, Waste Immobilization in Glass and Ceramic Based Hosts – Radioactive, Toxic and Hazardous Wastes, John Wiley & Sons Ltd., 2010.
[16] A. Abdelouas, S. Noirault, B. Grambow, J. Nucl. Mater. 358 (2006) 1–9.
[17] N.H. Hamodi, T.J. Abram, Int. J. Appl. Glass Sci. (2011).
[18] C.W. Sinton, W.C. LaCourse, Mat. Res. Bull. 36 (2001) 2471–2479.
[19] A.J. Connelly, R.J. Hand, P.A. Bingham, N.C. Hyatt, J. Nucl. Mater. 408 (2011) 188–193.
[20] C1285-02 Standard Test Methods for Determining Chemical Durability of Nuclear, Hazardous, and Mixed Waste Glasses and Multiphase Glass Ceramics: the Product Consistency Test (PCT), ASTM International, 2002.
[21] C1220-98 Standard Test Method for Static Leaching of Monolithic Waste Forms for Disposal of Radioactive Waste, ASTM International, 2004.
[22] D.L. Parkhurst, User's guide to PHREEQC-A computer program for speciation, reaction-path, advective-transport, and inverse geochemical calculations, US Geological Survey Water-Resources Investigations Report 95-4227, vol. 143, 1995.
[23] W.D. Kingery, Introduction to Ceramics, second ed., John Wiley & Sons, 1976.
[24] N. Rajmohan, P. Frugier, S. Gin, Chem. Geol. 279 (2010) 106–119.
[25] I.W. Donald, B.L. Metcalfe, R.N.J. Taylor, J. Mater. Sci. 32 (1997) 5851–5887.
[26] P.A. Bingham, R.J. Hand, O.M. Hannant, S.D. Forder, S.H. Kilcoyne, J. Non-Cryst. Solids. 355 (2009) 1526–1538.
[27] R.W. Revie, Uhlig's Corrosion Handbook, second ed., John Wiley & Sons, 2000.
[28] M. Todorović, L. Radonjić, Ceram. Int. 15 (1989) 383–388.
[29] P.K. Abraitis, F.R. Livens, J.E. Monteith, J.S. Small, D.P. Trivedi, D.J. Vaughan, R.A. Wogelius, Appl. Geochem. 15 (2000) 1399–1416.
[30] B.P. McGrail, W.L. Ebert, A.J. Bakel, D.K. Peeler, J. Nucl. Mater. 249 (1997) 175–189.
[31] E.M. Pierce, E.A. Rodriguez, L.J. Calligan, W.J. Shaw, B.P. McGrail, Appl. Geochem. 23 (2008) 2559–2573.
[32] R.J. Hand, P.A. Bingham, N.C. Hyatt, Glass Technol. Eur. J. Glass Sci. Technol. A. 53 (2012) 83–100.
[33] G.B. Alexander, W.M. Heston, R.K. Iler, J. Phys. Chem. 58 (1954) 453–455.
[34] X. Feng, I.L. Pegg, J. Non-Cryst. Solids. 175 (1994) 281–293.
[35] T. Geisler, A. Janssen, D. Scheiter, T. Stephan, J. Berndt, A. Putnis, J. Non-Cryst. Solids 356 (2010) 1458–1465.
[36] C.A. Utton, R.J. Hand, P.A. Bingham, N.C. Hyatt, S.W. Swanton, S.J. Williams, J. Nucl. Mater. 2012 (435) (2013) 112–122.
[37] C.A. Utton, S.W. Swanton, J. Schofield, R.J. Hand, A. Clacher, N.C. Hyatt, Min. Mag 76 (2012) 2919–2930.
[38] C.G. Pantano, G. Chen, D. Qi, Mater. Sci. Eng. A – Struct. 126 (1990) 191–201.